31555

by UMB IJIMEAM

Submission date: 06-Apr-2025 07:00PM (UTC+0700)
Submission ID: 2636584576
File name: 31555-89535-1-SM.docx (996.48K)
Word count: 5396
Character count: 29798

International Journal of Innovation in Mechanical Engineering and Advanced Materials
Vol. 1 (No. 1), 2024, pp. XX-XX
Journal homepage: publikasi.mercubuana.ac.id/index.php/ijimeam
DOI: 10.22441/ijimeam.v6i1.xxx

Analysis of Heat Transfer Enhancement Through Microchannels of Different Geometries

Soumik Kumar Hazra [1,*]

[1]Department of Mechatronical Engineering, Faculty of Engineering, University of Debrecen, Otemeto Utca 2-4, 4028, Debrecen, Hungary

Abstract

This study presents a comprehensive analysis of heat transfer enhancement in microchannels with varying geometries, focusing on wavy channels with trapezoidal cross-sections. The research aims to enhance the performance of electronic sinks by optimizing heat flux removal or maintaining a lower sink temperature with minimal pumping power. A three-dimensional numerical study of conjugate heat transfer is conducted using the Navier-Stokes equations, solved through the finite volume method. The SIMPLEC pressure correction scheme is applied to couple pressure and velocity fields. This study investigates wavy microchannels with trapezoidal cross-sections to improve heat transfer, utilizing water as the working fluid and silicone as the material of solid walls, and a comparative analysis is conducted between wavy channels with trapezoidal and rectangular cross-sections. The investigation evaluates the impact of cross-sectional geometry, particularly the top-to-bottom ratio (0.075–0.055 mm) on heat transfer and pressure drop, keeping the hydraulic diameter constant. Comparative results indicate superior heat transfer performance in trapezoidal wavy channels compared to rectangular ones, attributed primarily to enhanced relative waviness. An extensive parametric study has been carried out to identify the structure that produces the highest thermal performance. A distinctive contribution of this analysis is the identification of the underlying physics through a thorough analysis of the flow structures. This study highlights the critical role of geometric design in improving thermal management systems.

Article Info:
Received: xx xxx 2024
Revised: xx xxx 2024
Accepted: xx xxx 2024
Available online: xx xxx 2024

Keywords:
Microchannel heat sink (MCHS), Wavy microchannels, Trapezoidal, Heat transfer enhancement, Reynolds number, Nusselt number, Friction factor

1. Introduction

The current trend of miniaturization of electronic packages and increase in power density are the main reasons why traditional cooling approaches using fans are becoming impractical or unable to meet the increasing cooling demands of electronic devices. The critical bottleneck for the development of technically advanced electronic products is thermal issues [1]. According to the report published by the International Technology Roadmap for Semiconductors (ITRS), the reason behind peak power consumption was the ongoing COVID-19 pandemic when most people were forced to work from home due to safety reasons, and that boosted the sales of PCs by 11% in 2020. Overall growth of semiconductors is expected to continue in 2021 at a rate of 5% to 7%, which will raise the power consumption by 96% (147 W–288 W) in 2022 [2].

The ongoing research on microfabrication technology paved the way for designing microchannel heat sinks (MCHS) that are more useful and intricate than featureless, straight microchannels [3]. From the pioneering experimental study conducted by Tuckerman and Peace, which was performed by keeping the focus on cooling VLSI chips, the heat was removed at a rate of 790 W/cm² by water flowing through regular rectangular microchannels [4]. The high cooling rate was achieved due to a high ratio of surface area to volume of the microchannels. Later, this result was utilized in developing other electronic and laser applications with better heat management systems. Deionized water is the most popular liquid coolant due to its low cost, availability, and longevity. The maximum optimum temperature in electronic devices should be kept below its boiling point, rendering the flow to be in the liquid phase only. Three-dimensional Navier–Stokes equations in terms of liquid-phase conjugate heat transfer modeling were used successfully for MCHS design analyses in the past. Earlier studies considered different heat sink dimensions, variations of fluid properties, channel roughness, and boundary conditions [5]-[7]. The close matching be-

tween experimental results and numerical predictions was attributed to remarkable improvement in analogy and measurements over the last 30 years or so [8]. Experiments confirmed that the effect of relative roughness less than 10-5 is negligible. In numerical models, the necessity of incorporating appropriate variations of fluid property with temperature variation was established earlier by several researchers. Previous simulations that involved conjugate heat transfer revealed an increase in heat transfer of about 11.7% for a bottom wall thickness of 250 µm concerning an analysis conducted by ignoring this thickness and by about 20% for using copper instead of silicon for the wall material. Of course, the predicted increases have arisen due to the modeled heat conduction in the vertical and axial directions through the solid [3]. If the wall of a microchannel wall remains featureless, the boundary layer continuously grows and impedes heat transfer.

One remarkable solution is direct liquid cooling incorporating microchannels [9], [10]. Relevant studies related to this research include both single-phase cooling and two-phase (boiling) cooling. Two-phase has a potentially higher heat removal capacity, but it involves complex issues such as condensation, saturation temperature, critical heat flux, nucleation site activation, etc. [3]. The work of Tuckerman and Peace for electronic cooling sparked tremendous research interests in the application of microchannel-based heat sinks. Design variations and material properties significantly influence the heat transfer enhancement in microchannels [11]. A conventional microchannel heat sink generally employs straight channels in which the streamlines of the coolant are nearly straight, due to which the heat transfer is inefficient and resultant fluid mixing is poor. This results in temperature gradients across the integrated circuit (IC) chip, exacerbated by boundary layer thickening along the flow path, which diminishes heat transfer performance downstream. Non-uniform heat flux distributions on the chip surface further compound this issue, creating localized hot spots that conventional designs struggle to mitigate. Such thermal non-uniformities negatively impact IC reliability and can precipitate premature failure. Consequently, there is a strong imperative to improve microchannel heat sink performance without incurring substantial increases in pumping power or resorting to complex three-dimensional microstructures that pose manufacturing challenges. So, the proposal of bringing changes in the design of microchannels by changing the dimensions e.g. semi-octagonal rectangular microchannel or by introducing cavities in the shape like wavy, reentrant, etc. has shown certain improvements in the heat transfer of the channel [12]-[15]. On the other hand, along with heat transfer, the pressure drop is also an important factor that determines the practicability of the design for real-world application. Improvement in heat transfer performance usually increases pressure drop and pumping power. From the numerical analysis of fluid flow and heat transfer characteristics of the novel microchannel heat sink, studies have revealed that a favorable balance between heat transfer and pressure drop can enhance the potential for high heat transfer and efficiency of a microchannel [16]-[18].

In this work, the goal was to thoroughly investigate the nature and change of heat transfer through different shapes of microchannels (simple and wavy, both) keeping the boundary conditions and hydraulic diameter the same. The focus was to investigate the difference in heat transfer rate through microchannels of rectangular (simple and wavy) and trapezoidal (simple and wavy) shapes of various dimensions.

2. Methods

Some assumptions were made in modeling the heat transfer in microchannels to simplify the analysis: a) Steady state b) Laminar flow c) Incompressible fluid d) negligible viscous dissipation e) constant fluid properties f) negligible radiative and natural convective heat transfer from the microchannel heat sink. The assumptions made to analyse the heat transfer due to water flow through an MCHS made of silicon are as follows-

a) Water is behaving as Newtonian and incompressible fluid, and the flow is laminar [19].
b) Radiation heat transfer and gravity force have been neglected.
c) The effect of Viscous dissipation has been ignored.
d) Piecewise linear variation of thermal conductivity and viscosity of water with temperature has been employed [20].
e) The effect of EDL is ignored as the hydraulic diameter in all the cases considered here are far greater than 40 µm, above which the effect becomes insignificant [21].

All the important terms necessary for the mathematical formulations and defining of equations related to the study have been presented in Table 1.

Table 1. Nomenclature

A = area m^2	Nu = Nusselt number	D = Hydraulic mean diameter of channel
C_p = specific heat J $kg^{-1}K^{-1}$	Re = Reynolds number	Q = Total Heat transfer
H = heat transfer coefficient W m^{-2} K^{-1}	T = temperature	Tw = temp of the bottom wall
Lc = overall length of the microchannel	x, y, z = three coordinates	Tf = temp of the flowing water
m = mass flow rate of water kg s^{-1}	Wc = Width of the channel	P_{inlet}= inlet pressure
F = Friction factor	Hc = Height of the channel	P_{outlet}= outlet pressure

2.1. Description of the problem geometry

In the present study,8 different types of microchannels with different dimensions, shapes, and properties have been considered to study the effects of different hydraulic diameters on wavy microchannels (rectangular and trapezoidal), consequences of changing aspect ratio of trapezoidal channels with the same hydraulic diameter and to do a thorough comparison of heat transfer.

Fig:1(a) is a representation of a simple rectangular microchannel subjected to constant heat flux at the bottom wall made of silicon and water is used as a working fluid within the microchannels. The domain is labeled by a total length(L) of 10mm, Width(W) of 0.3mm, and Height(H) of 0.35mm. The microchannel width (Wc) is 0.1mm and the channel height (Hc) is 0.2mm. The hydraulic mean diameter of the channel (D) is taken as 133µm. Fig:1(b) represents a wavy rectangular microchannel of domain length(L), width(W), and height(H) same as the simple rectangular microchannel depicted by Fig: 1(a) with 4 full waves of each wave amplitude (A) being 2.5mm. The microchannel height (Hc) and width (Wc) whose adopted values are 0.2mm and 0.1mm respectively. The hydraulic mean diameter (D) of the channel has been kept as same as the simple rectangular microchannel.

Fig:2-4 are the representations of simple trapezoidal and wavy trapezoidal channels respectively which have been considered for the study by varying different dimensions/parameters. 3 simple trapezoidal and 3 wavy trapezoidal channels have been taken whose total domain length(L), height(H), and width(W) are 10mm,0.35mm, and 0.3mm. The wave amplitude (A) of the full waves depicted is 2.5 mm. For the first simple and wavy trapezoidal channels depicted in Fig:2(a) and Fig:2(b) respectively, microchannel base/bottom width (Wcb) of 0.075mm, top width (Wct) of 0.125mm, microchannel height (Hc) of 0.2mm have been considered. From Fig:3(a) and Fig:3(b), it is visible that the second simple and wavy trapezoidal channels have a microchannel base/bottom width (Wcb) of 0.055mm, top width (Wct) of 0.15mm, microchannel height (Hc) of 0.2mm. Both channels have a hydraulic diameter of 133µm. Third simple and wavy trapezoidal channels indicated by Fig:4(a) and Fig:4(b) respectively, have been taken by varying the hydraulic diameter to 144µm and having channel top width (Wct) of 0.18mm, channel base/bottom width (Wcb) of 0.055mm, channel height (Hc) of 0.2mm.

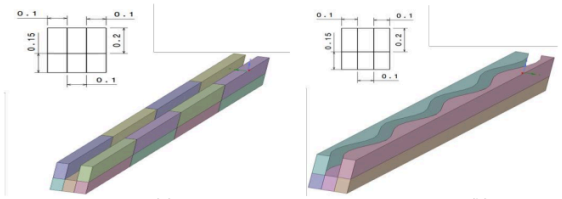

(a) (b)

Figure 1. Microchannel, (a) Simple Rectangular (b) Wavy

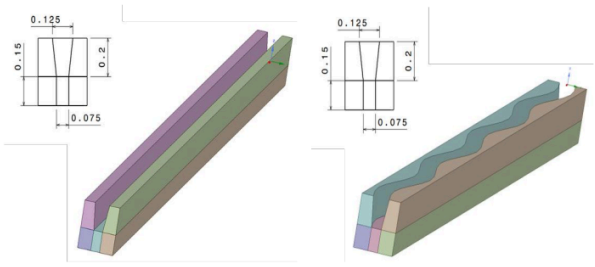

(a) (b)

Figure 2. Trapezoidal (0.075 mm base) Channel, (a) Simple (b) Wavy

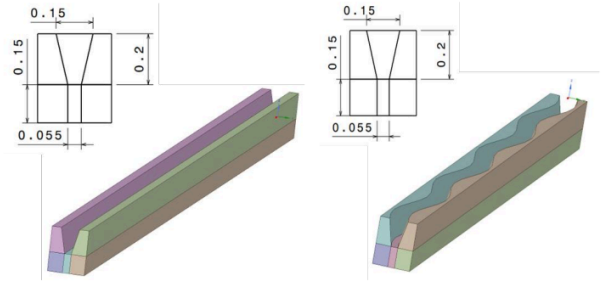

(a) (b)

Figure 3. Trapezoidal (0.055 mm base) Channel, (a) Simple (b) Wavy

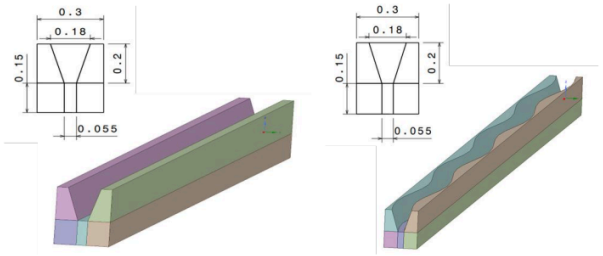

(a) (b)

Figure 4. Trapezoidal (0.18 mm top) Channel, (a) Simple (b) Wavy

The wavy line has been represented by the equation y = A cos(2px/L), where A represents the wave amplitude, and L represents the wavelength. In this study, the real computational domain of one wavy microchannel consists of at least 10 to 12 wavy units with changing or constant relative wavy amplitude. The thermal and hydrodynamic performance of these wavy microchannels has been studied and compared with baseline microchannels, both having the same cross sections and total lengths. For simulations under constant wall temperature (T) and constant wall heat flux conditions, the x–y plane reflection symmetry allows it to be carried out in only one-half of the real geometry. In the conjugate simulation, silicon has been considered as substrate material, since heat flux in the substrate can be well approximated to be relatively uniform because of its high thermal diffusivity. Numerical simulations were conducted using the commercial computational fluid dynamics (CFD) software package ANSYS FLUENT 16, employing a finite-volume approach to solve the steady, incompressible Navier-Stokes equations. Pressure discretization utilizing the standard scheme was applied, while the SIMPLE algorithm addressed pressure-velocity coupling. Second-order upwind discretization was applied to both the momentum and energy equations. Implementation of heat transfer (H2) and thermal (T) boundary conditions on the microchannel walls was performed directly within FLUENT. For conjugate heat transfer simulations, a uniform heat flux was imposed on the bottom surface of the silicon substrate, with an adiabatic condition applied to the upper surface. Periodic boundary conditions were implemented on the lateral exterior surfaces. Recognizing the significant influence of flow boundary conditions on velocity profiles and heat transfer characteristics, particularly in complex geometries such as wavy channels, a uniform velocity profile was specified at the channel inlet, an outflow condition at the outlet, and no-slip conditions at the channel walls. The coolant (liquid water) inlet temperature was maintained at 293 K and the inlet wall temperature was also the same. Additionally, a heat flux of 1000000 W/m^2 at the bottom wall has been given. Convergence absolute criteria values for continuity and energy equations have been considered as 1e-06 and 1e-08 respectively.

2.2. Numerical Formulation

The governing equations for conservation of mass, momentum, and energy for the liquid and the energy equation for the solid are represented by the following equations –

$$\frac{\partial u_i}{\partial x_i} = 0 \tag{1}$$

$$\frac{\varrho_f \partial u_i}{\partial t} + \frac{\varrho_f u_j \partial u_i}{\partial x_j} = -\frac{\partial p}{\partial x_i} + \frac{\partial\left\{\left(\frac{\partial u_j}{\partial x_i} + \frac{\partial u_i}{\partial x_j}\right)\right\}}{\partial x_j} \tag{2}$$

$$\frac{\varrho_f C_f \partial T}{\partial t} + \frac{\varrho_f C_f u_i \partial T}{\partial x_i} = -\frac{\partial\left(\frac{K_f \partial T}{\partial x_i}\right)}{\partial x_i} \quad (3)$$

$$\frac{\varrho_s C_s \partial T}{\partial t} = -\frac{K_s \partial T^2}{\partial x_i^2} \quad (4)$$

where i,j = 1,2,3,...n

The applied boundary conditions are-

a) At the inlet side (X = 0), constant flow velocity ($u = u_{in}$, v = w = 0) and temperature (T= 293 K) has been applied.

b) At the outlet side (X=L), the fluid pressure and temperature are specified as $p|_{x=L} = p_{out} = 0$ and $(\partial T/\partial x)|_{x=L} = 0$ [23].

c) For the solid wall at the inlet and exit sides (at X = 0 and X= L) , insulated condition is given by ∂T/∂x = 0, following the existing practice [23],[24].

d) The top surface (z = H) of a heat sink is generally covered by pyrex plate. So, insulated heat transfer condition is adopted by $(\partial Ts/\partial z)|_{z=H} = 0$ as a reasonable assumption.

e) At the bottom wall (z= 0), constant heat flux (10^6 W/m²) is given by $-ks(\partial Ts/\partial z) = q = 10^6$ W/m².

f) At the fluid–solid interface, no slip condition, no penetration and equal temperature are given as u = v = w = 0 and Ts = Tf .

g) At the two opposite sides of the channel (y = 0 and y = W), the symmetry conditions are given by ∂T/∂y = 0, ∂u/∂y = 0, and v = w = 0 due to periodicity.

h) Total bottom area of the channel = 0.3 x Lc

i) Total Heat transfer (Q) = 1000000 watt/m² x Bottom wall area

Reynolds number is calculated by the velocity of fluid u_{in}, hydraulic diameter D_h as

$$Re = (\varrho_{f,in} D_h u_m)/\mu_{f,avg} \quad (5)$$

Hydraulic mean diameter and weighted area of the channel are calculated by following equations:

$$D = \frac{2 \times (Wc \times Hc)}{(Wc + Hc)} \quad (6)$$

$$W = \frac{Wc \times Lc}{2(Hc \times Lc)} \quad (7)$$

Convective Heat transfer coefficient, Nusselt Number, and Friction factor are calculated by:

$$h = \frac{Q}{(weighted\ area \times (Tw - Tf))} \quad (8)$$

$$Nu = \frac{(D \times h)}{(K_{water\ at\ Tf})} \quad (9)$$

$$f = \frac{(2 \times (P_{inlet} - P_{outlet}) \times D)}{(\varrho_f \times (u_{in})^2 \times L)} \quad (10)$$

2.3. Grid Independency Test

Grid independency test has been carried out to find out the suitable mesh size for the analysis. We have compared the mesh with 800000 grids and 1200000 grids and observed that there is no significant change in results between these two mesh. Table 3 shows the relative error in Nusselt number and friction factor at different grid numbers for wavy trapezoidal microchannel for inlet velocity of 2 m/sec. The percentage error is calculated by differentiating m1 from m2 and

by doing percentage calculation upon m1 where m represents any parameter such as Nusselt number and friction factor, m1 represents finest grids and m2 represents coarse grids. From the analysis it is evident that,800000 grids are enough for our further calculations.

3. Results and Discussion

This study investigates the enhancement of heat transfer in trapezoidal microchannels by introducing sinusoidal wall undulations. Four distinct cross-sectional geometries were analyzed: one rectangular and three trapezoidal configurations of varying dimensions, to assess the impact of this geometric modification on heat transfer performance. The specific waveform geometry is detailed in the geometry description section. All simulations assumed a silicon microchannel material with constant specific heat (702 J/kg·K) and thermal conductivity (148 W/m·K), with water as the coolant. Inlet water velocity was varied from 0.5 m/s to 4 m/s to explore the influence of Reynolds number (Re) on heat transfer. The Nusselt number (Nu) was employed as the primary metric for evaluating heat transfer efficiency, with higher Nu values indicating improved performance. The study also examined the potential influence of hydraulic diameter on heat transfer enhancement in the wavy channel configurations by including a cross-section with a distinct hydraulic diameter. Numerical simulations were performed using ANSYS 16.0 to determine bottom wall temperatures, coolant temperatures, and inlet/outlet pressures, which were subsequently used to calculate Nusselt numbers. The following sections present a detailed analysis of the observed heat transfer enhancement across the different cross-sectional geometries.

3.1. Rectangular Cross-section

Initially, a rectangular microchannel with a hydraulic diameter of 0.133 mm, was analyzed. Simulations of the smooth channel configuration revealed a direct correlation between Reynolds number and heat transfer, with increasing Re leading to enhanced heat transfer. Concurrently, pressure drop across the channel increased, while the friction factor decreased. Upon transitioning from a smooth to a wavy channel geometry, a more pronounced increase in Nusselt number with increasing Re was observed, as illustrated in Figure 5. This indicates that the heat transfer enhancement becomes more significant at higher inlet water velocities which is tabulated below in table 2 and 3. Also Nu/Nu_0 against Re graph has been plotted to validate the heat transfer enhancement (Figure 6).

Table 2. Analysis for simple rectangular microchannel

Inlet Velocity (m/s)	Tw (in K)	Tf (in K)	Inlet P	Outlet P	h at Tf	Nu	Friction factor (f)
0.5	346.94	323.43	4706.99	170.60	25521.24	5.25	0.485
1	331.10	308.39	11846.75	659.78	26411.55	5.62	0.299
1.5	325.17	303.36	20019.09	1470.40	27504.84	5.93	0.220
2	321.79	300.83	28980.30	2600.15	28617.99	6.23	0.176
2.5	319.50	299.30	38630.93	4048.71	29693.71	6.49	0.148
3	317.81	298.27	48927.52	5816.61	30713.08	6.74	0.128
3.5	316.48	297.54	59855.50	7907.80	31676.86	6.98	0.113
4	315.39	296.98	71396.35	10319.99	32591.43	7.19	0.102

Table 3. Analysis for wavy rectangular microchannel

Inlet Velocity (m/s)	Tw (in K)	Tf (in K)	Inlet P	Outlet P	h at Tf	Nu	Friction factor (f)
0.5	346.45	324.09	4842.72	171.45	26831.27	5.51	0.4992
1	330.05	308.75	12349.45	666.44	28168.58	5.99	0.3121
1.5	323.47	303.60	21179.21	1487.81	30208.27	6.52	0.2338
2	319.41	301.00	31114.10	2632.44	32581.92	7.10	0.1902
2.5	316.49	299.41	42078.73	4097.86	35136.50	7.68	0.1623
3	314.23	298.35	54032.10	5877.64	37781.47	8.29	0.1429
3.5	312.43	297.59	66984.33	7965.78	40417.21	8.91	0.1287

4	310.99	297.02	80953.34	10359.69	42954.40	9.48	0.1179

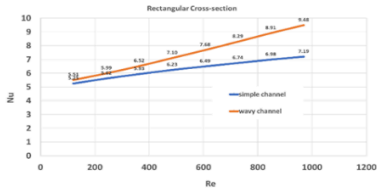

Figure 5. Change in ratio of Nusselt number in wavy and smooth rectangular channel with Re

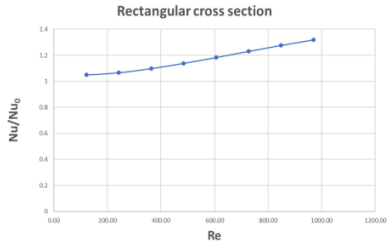

Figure 6. Nu/Nu_0 vs Re plot for rectangular channel

3.2. Trapezoidal (0.075 mm base) Cross-section

To investigate potential alterations in heat transfer enhancement characteristics, the rectangular cross-section was modified to a trapezoidal geometry while maintaining a constant hydraulic diameter of 0.133 mm. This was achieved by reducing the bottom edge length from 1 mm to 0.75 mm and adjusting the top edge length accordingly (cross-sectional details are provided in the geometric description section). Using identical simulation parameters as the rectangular channel analysis, both smooth and wavy trapezoidal configurations were evaluated. While the overall heat transfer decreased due to the reduction in bottom edge length as depicted by Figure 7, the primary objective was to determine if the transition from a smooth to a wavy channel resulted in a different heat transfer enhancement pattern compared to the rectangular case. Table 4 and 5 provides a detailed result of the analysis. From the Nu/Nu_0 vs Re plot of Figure 8, we can see that there is not so much change in the heat transfer enhancement pattern in trapezoidal cross section.

Table 4. Analysis for simple trapezoidal (0.075 mm base) microchannel

Inlet Velocity (m/s)	Tw (in K)	Tf (in K)	Inlet P	Outlet P	h at Tf	Nu	Friction factor (f)
0.5	348.53	323.35	4798.90	169.19	24918.26	5.11	0.493
1	332.50	308.36	12056.38	656.93	25990.87	5.51	0.304
1.5	326.43	303.35	20381.47	1468.65	27179.82	5.85	0.224
2	322.95	300.82	29500.02	2601.79	28352.97	6.16	0.179
2.5	320.59	299.29	39328.30	4058.30	29465.98	6.42	0.150
3	318.83	298.27	49816.12	5837.53	30513.28	6.67	0.130
3.5	317.46	297.53	60940.20	7940.06	31497.32	6.92	0.115

4	316.33	296.98	72686.77	10368.04	32424.48	7.14	0.104

Table 5. Analysis for wavy trapezoidal (0.075 mm base) microchannel

Inlet Velocity (m/s)	Tw (in K)	Tf (in K)	Inlet P	Outlet P	h at Tf	Nu	Friction factor (f)
0.5	347.807	323.736	4894.515	169.977	26066.915	5.35	0.504
1	331.136	308.586	1246.792	660.558	27825.508	5.90	0.315
1.5	324.396	303.500	2137.245	1475.739	30028.229	6.46	0.236
2	320.247	300.925	3137.203	2612.924	32473.581	7.06	0.192
2.5	317.271	299.362	4238.849	4067.637	35036.321	7.64	0.163
3	314.980	298.312	5438.943	5835.501	37645.724	8.24	0.144
3.5	313.156	297.560	6734.652	7909.449	40231.107	8.84	0.129
4	311.675	296.995	8128.118	10286.619	42741.781	9.41	0.118

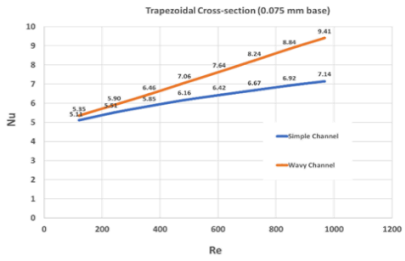

Figure 7. Change in ratio of Nusselt number in wavy and smooth trapezoidal channel(0.075mm base) with Re

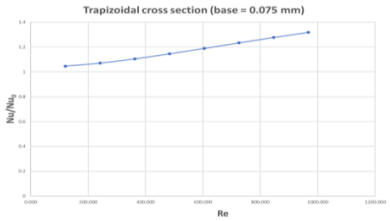

Figure 8. Nu/Nu_0 vs Re plot for trapezoidal (0.075mm base) channel

3.3. Trapezoidal (0.055 mm base) Cross-section

Prior observations demonstrated an insignificant variation in heat transfer augmentation within the microchannels when the MCHS configuration transitioned from a smooth to a wavy profile. To investigate the impact of trapezoidal geometry on heat transfer enhancement while maintaining a constant hydraulic diameter, an alternative trapezoidal cross-section was employed. This modification involved reducing the bottom edge length to 0.055 mm and adjusting

the top edge length accordingly to preserve the hydraulic diameter. The analytical results aligned with expectations (from Table 6 and 7), revealing no appreciable improvement in heat transfer between smooth and wavy-shaped microchannels and the changes have been shown by Figure 9. It is also visible from the Figure 10 that the Nu/Nu_0 Vs Re plot was almost same as the previous two cases.

Table 6. Analysis for simple trapezoidal (0.055 mm base) microchannel

Inlet Velocity (m/s)	Tw (in K)	Tf (in K)	Inlet P	Outlet P	h at Tf	Nu	Friction factor (f)
0.5	349.943	322.496	4745.789	170.999	23448.888	4.82	0.488
1	333.808	307.955	1190.497	662.539	24895.391	5.29	0.300
1.5	327.552	303.077	2013.712	1481.589	26296.307	5.66	0.221
2	323.932	300.617	2917.288	2625.768	27605.525	6.00	0.177
2.5	320.59	299.131	3892.187	4097.599	28810.501	6.28	0.148
3	319.641	298.134	4934.151	5896.754	29926.018	6.55	0.129
3.5	318.204	297.419	6040.776	8023.043	30963.995	6.81	0.114
4	317.033	296.880	7211.215	10478.391	31935.305	7.03	0.103

Table 7. Analysis for wavy trapezoidal (0.055 mm base) microchannel

Inlet Velocity (m/s)	Tw (in K)	Tf (in K)	Inlet P	Outlet P	h at Tf	Nu	Friction factor (f)
0.5	349.1017	323.2936	4868.275	177.023	24938.06	5.12	0.500
1	332.3624	308.3987	1237.916	682.492	26857.39	5.70	0.312
1.5	325.4955	303.4059	2120.346	1520.382	29135.93	6.27	0.233
2	321.2258	300.8629	3111.374	2686.804	31606.5	6.87	0.189
2.5	318.1524	299.3092	4201.004	4176.030	34155.69	7.45	0.161
3	315.8274	298.2626	5384.813	5983.292	36641.65	8.02	0.142
3.5	314.0094	297.5125	6657.124	8099.100	39013.38	8.58	0.127
4	312.5441	296.6504	8020.204	10522.583	40494.06	8.92	0.116

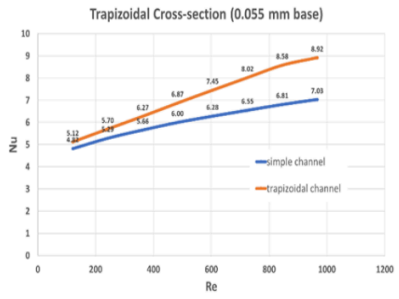

Figure 9. Change in ratio of Nusselt number in wavy and smooth trapezoidal channel(0.055mm base) with Re

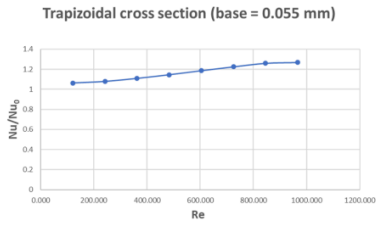

Figure 10. Nu/Nu_0 vs Re plot for trapezoidal (0.055mm base) channel

3.4. Trapezoidal (0.18 mm top) Cross-section

To evaluate the influence of hydraulic diameter on heat transfer enhancement while transitioning the MCHS from a smooth to a wavy configuration, a distinct trapezoidal channel with a hydraulic diameter of 0.144 mm was introduced. The top width was maximized within the constraints of accommodating both smooth and wavy channel configurations within the limited width of a single MCHS unit. Detailed geometric specifications are elaborated upon in the geometric description section. The analytical findings (see Table 8 and 9) unequivocally demonstrate that variations in channel hydraulic diameter exert no discernible impact on the heat transfer enhancement pattern during the transition from a smooth to a wavy channel profile. As observed in prior instances, heat transfer increases with rising water inlet velocity in both smooth and wavy channel configurations. However, heat transfer augmentation is more pronounced with increasing Reynolds number when transitioning from a smooth to a wavy profile (reference Figure 11). Nu/Nu_0 Vs Re plot from Figure 12, is almost same as the previous cases indicating that the hydraulic diameter is not affecting the heat transfer enhancement pattern microchannels.

Table 8. Analysis for simple trapezoidal (0.18 mm top) microchannel

Inlet Velocity (m/s)	Tw (in K)	Tf (in K)	Inlet P	Outlet P	h at Tf	Nu	Friction factor (f)
0.5	348.4972	318.4165	4183.59	174.20	21037.03	4.67	0.462
1	333.6793	305.916	110448.61	674.91	22793.15	5.23	0.281
1.5	327.6832	301.711	217662.34	1505.95	24365.03	5.67	0.207
2	324.1465	299.588	25622.89	2666.01	25767.49	6.05	0.165
2.5	321.7166	298.304	234270.57	4156.98	27028.86	6.37	0.139
3	319.8983	297.442	943568.79	5979.04	28180.77	6.66	0.120
3.5	318.4631	296.824	453495.23	8132.11	29244.34	6.95	0.107
4	317.2883	296.358	464035.67	10616.09	30234.69	7.19	0.096

Table 9. Analysis for wavy trapezoidal (0.18 mm top) microchannel

Inlet Velocity (m/s)	Tw (in K)	Tf (in K)	Inlet P	Outlet P	h at Tf	Nu	Friction factor (f)
0.5	347.8324	319.348	4402.334	186.68973	22216.00	4.93	0.486
1	332.527	306.256	211292.53	716.170626	24087.94	5.52	0.305
1.5	325.5687	301.982	619584.88	1585.84036	26829.76	6.24	0.230
2	321.6665	299.901	29146.65	2791.39119	29073.97	6.83	0.190
2.5	318.3624	298.612	539924.29	4317.6392	32041.15	7.55	0.164
3	315.925	297.805	451889.38	6155.82136	34924.03	8.26	0.146
3.5	313.967	296.964	64974.5	8287.02453	37217.52	8.84	0.133
4	312.389	296.106	79220.42	10705.8233	38863.20	9.25	0.123

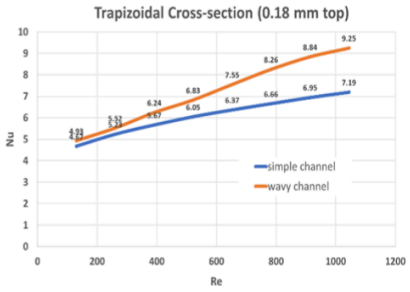

Figure 11. Change in ratio of Nusselt number in wavy and smooth trapezoidal channel(0.18mm top) with Re

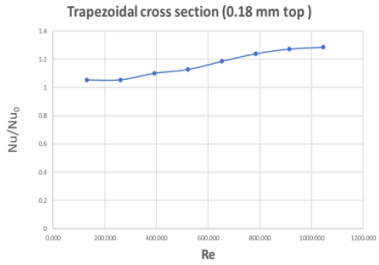

Figure 12. Nu/Nu_0 vs Re plot for trapezoidal (0.18mm top) channel

4. Conclusions

This study presents a computational fluid dynamics (CFD) investigation of laminar liquid-water flow and heat transfer within three-dimensional wavy microchannels with rectangular cross-sections. Simulations were conducted under constant wall heat flux and conjugate boundary conditions. The results demonstrate that these wavy microchannels exhibit sustained high levels of heat transfer performance along the flow direction, leading to significant overall heat transfer enhancement while incurring a minimal pressure drop penalty compared to straight microchannels. From the analysis, it can be clearly seen that for all the cases heat transfer is increasing with an increase in Reynold's number. But for the wavy channel, this increment is more rapid compared to the smooth channels. When the ratio of the Nusselt number for the smooth channel to the Nusselt number for the wavy channel for the same cross-section (Nu/Nu_0) has been plotted against Reynold's Number (Re), it shows that for all the channels Nusselt number ratio is increasing with Re and for all the cross sections the Nu/Nu_0 Vs Re plot is almost same which clearly indicates that heat transfer is increasing when the microchannel shape is changed from smooth to wavy. This enhancement in heat transfer is almost the same for a rectangular and trapezoidal cross-section of the channel when the hydraulic diameter of the cross-section has not been changed which means the channel cross-section has no effect on the heat transfer enhancement when the channel shape is changed from smooth to wavy. This finding is consistent with previous observations that variations in hydraulic diameter or the transition from smooth to wavy profiles have minimal impact on heat transfer enhancement patterns.

References

[1] C. T., P. L. Y. C. C. S. Y. Sui, "Fluid flow and heat transfer in wavy microchannels," International Journal of Heat and Mass Transfer, p. 2760–2772, 2010.

[2] I. I. F. T. International Roadmap Committee, "THE INTERNATIONAL ROADMAP FOR DEVICES AND SYSTEMS," IEEE, virtually held on International Symposium on Roadmapping Devices and Systems (2021 ISRDS), 2021.

[3] D. D. B. S. K. D. Aparesh Datta, "The Role of Flow Structures on the Thermal Performance of Microchannels with Wall Features," Journal of Thermal Science and Engineering Applications, vol. 13, no. 1.4047709, pp. 021019-1, 2020.

[4] D. B. a. P. R. F. Tuckerman, "High Performance Heat Sinking for VLSI," IEEE Electron Device Lett., vol. 2, no. 5, p. 126–129, 1981.

[5] W. M. I. Qu, "Experimental and Numerical Study of Pressure Drop and Heat Transfer in a Single-Phase Micro-Channel Heat Sink," Int. J. Heat Mass Transfer, vol. 45, no. 12, p. 2549–2565., 2002.

[6] H. Y. a. C. P. Wu, "An Experimental Study of Convective Heat Transfer in Silicon Microchannels With Different Surface Conditions," Int. J. Heat Mass Transfer, vol. 46, no. 14, p. 2547–2556, 2003.

[7] K. C. C. X. Y. a. C. J. C. Toh, "Numerical Computation of Fluid Flow and Heat Transfer in Microchannels," Int. J. Heat Mass Transfer, vol. 45, no. 26, p. 5133–5141., 2002.

[8] G. F.-M. M. a. A. D. Gamrat, "Conduction and Entrance Effects on Laminar Liquid Flow and Heat Transfer in Rectangular Microchannels," Int. J. Heat Mass Transfer, vol. 48, no. 14, p. 2943–2954, 2005.

[9] J. S. H. L. K. C. M.K. Kang, "Analysis of laminar convective heat transfer in micro heat exchanger for stacked multi-chip module," Microsyst.Technol., vol. 11, no. 18, p. 1176–1186, 2005.

[10] S. G. D. L. P.S. Lee, "Experimental investigation of heat transfer in microchannels," Int. J. Heat Mass Transfer, vol. 48, no. 16, p. 1688–1704, 2005.

[11] V. K. Pandey, V. Choudhary, C. Ranganayakulu, and A. A. M., "Thermal Hydraulic Performance and Characteristics of a Microchannel Heat Exchanger: Experimental and Numerical Investigations," *ASME Journal of Heat and Mass Transfer*, vol. 147, no. 2, Nov. 2024, doi: 10.1115/1.4067012.

[12] M. N. Akram, K. Mohiuddin, M. A. S. Akash, F. Ibeh, and M. S. Kibria, "Numerical Investigation on Enhanced Thermal Performance of Rectangular Microchannels with Triangular Ribs", *AAES*, pp. 1–11, Sep. 2024, doi: 10.47852/bonviewAAES42023989.

[13] T. Yu, X. Guo, and Y. Tang, "Numerical investigations of heat transfer augmentation in a microchannel heat sink with different shaped periodic reentrant cavities on channel sidewalls," *Can J Phys*, vol. 102, no. 11, pp. 590–603, Jul. 2024, doi: 10.1139/cjp-2023-0275.

[14] D. K. Raj, A. Datta, and N. K. Soni, "Design of the Microchannels Heat Sink to Augment the Thermal Performance Using Different Type of Cavity with or without Wavy Channel," *Heat Transfer Engineering*, pp. 1–18, doi: 10.1080/01457632.2024.2317605.

[15] Q. Wang, J. Tao, Z. Cui, T. Zhang, and G. Chen, "Passive enhanced heat transfer, hotspot management and temperature uniformity enhancement of electronic devices by micro heat sinks: A review," *Int J Heat Fluid Flow*, vol. 107, p. 109368, 2024, doi: https://doi.org/10.1016/j.ijheatfluidflow.2024.109368.

[16] M. A. Wazir, K. Akhtar, U. Ghani, M. Wajib, S. Shaukat, and H. Ali, "Thermal enhancement of microchannel heat sink using pin-fin configurations and geometric optimization," *Engineering Research Express*, vol. 6, no. 1, p. 015526, 2024, doi: 10.1088/2631-8695/ad3400.

[17] S. Ahmed Memon, S. Akhtar, T. Ahmad Cheema, and C. Woo Park, "Enhancing heat transfer in microchannels: A systematic evaluation of crescent-like fin and wall geometries with secondary flow," *Appl Therm Eng*, vol. 239, p. 122099, 2024, doi: https://doi.org/10.1016/j.applthermaleng.2023.122099.

[18] Yew Wai Loon, Nor azwadi Che Sidik, and Yutaka Asako, "Numerical Analysis of Fluid Flow and Heat Transfer Characteristics of Novel Microchannel Heat Sink", *J. Adv. Res. Numer. Heat Trans.*, vol. 15, no. 1, pp. 1–23, Dec. 2023.

[19] W. Qu, I. Mudawar, Experimental and numerical study of pressure drop and heat transfer in a single-phase micro-channel heat sink, Int. J. Heat Mass Tran. 45 (2002) 2549–2565.

[20] G. Xia, Y. Zhai, Z. Cui, Numerical investigation of thermal enhancement in a micro heat sink with fan-shaped reentrant cavities and internal ribs, Appl. Therm. Eng. 58 (2013) 52–60

[21] I.A. Ghani, N. Kamaruzaman, N.A.C. Sidik, Heat transfer augmentation in a microchannel heat sink with sinusoidal cavities and rectangular ribs, Int. J. Heat Mass Tran. 108 (2017) 1969–1981.

[22] Y.F. Li, G.D. Xia, D.D. Ma, Y.T. Jia, J. Wang, Characteristics of laminar flow and heat transfer in microchannel heat sink with triangular cavities and rectangular ribs, Int. J. Heat Mass Tran. 98 (2016) 17–28.

[23] G. Xia, L. Chai, H. Wang, M. Zhou, Z. Cui, Optimum thermal design of microchannel heat sink with triangular reentrant cavities, Appl. Therm. Eng. 31 (2011) 1208–1219

[24] G. Xia, L. Chai, M. Zhou, H. Wang, Effects of structural parameters on fluid flow and heat transfer in a microchannel with aligned fan-shaped reentrant cavities, Int. J. Therm. Sci. 50 (2011) 411–419

31555

ORIGINALITY REPORT

14%	10%	14%	4%
SIMILARITY INDEX	INTERNET SOURCES	PUBLICATIONS	STUDENT PAPERS

PRIMARY SOURCES

1	Submitted to United International University Student Paper	3%
2	coek.info Internet Source	3%
3	K Bala Subrahmanyam, Pritam Das, Aparesh Datta. "Numerical investigation on fluid flow and convective heat transfer in a microchannel heat sink with fan-shaped cavities and ribs", Proceedings of the Institution of Mechanical Engineers, Part E: Journal of Process Mechanical Engineering, 2021 Publication	2%
4	Aparesh Datta, Vivek Sharma, Dipankar Sanyal, Pritam Das. "A conjugate heat transfer analysis of performance for rectangular microchannel with trapezoidal cavities and ribs", International Journal of Thermal Sciences, 2019 Publication	1%
5	aip.scitation.org Internet Source	1%
6	atsla.cau.ac.kr Internet Source	1%
7	semarakilmu.com.my Internet Source	1%
8	publications.waset.org Internet Source	<1%
9	Sui, Y., C. J. Teo, P. S. Lee, Y. T. Chew, and C. Shu. "An Efficient Wavy Microchannel Heat Sink for Electronic Devices", Volume 1 Heat	<1%

	Transfer in Energy Systems Thermophysical Properties Heat Transfer Equipment Heat Transfer in Electronic Equipment, 2009. Publication	
10	Lei Chai, Liang Wang, Xin Bai. "Thermohydraulic performance of microchannel heat sinks with triangular ribs on sidewalls – Part 2: Average fluid flow and heat transfer characteristics", International Journal of Heat and Mass Transfer, 2019 Publication	<1 %
11	etheses.whiterose.ac.uk Internet Source	<1 %
12	html.pdfcookie.com Internet Source	<1 %

Exclude quotes	On	Exclude matches	< 17 words
Exclude bibliography	On		